Vacuum 190 (2021) 110295

Contents lists available at ScienceDirect

Vacuum

journal homepage: www.elsevier.com/locate/vacuum

Functionalization of microfluidic devices by microstructures created with proton beam lithography

Emad Nady, Gyula Nagy, Róbert Huszánk *

Institute for Nuclear Research (Atomki), H-4001, Debrecen, P.O. Box 51, Hungary

ARTICLE INFO

Keywords:
Proton beam writing
Microfluidics
Microfluidic passive mixers

ABSTRACT

Microfluidic devices have become important part of technology nowadays in numerous fields of application, such as chemical reactions, biosensors, synthesis of nanomaterials, diagnostic device for detection of biological samples, etc.

In this work, as a new fabrication approach, poly(dimethyl-siloxane) (PDMS) microstructures were integrated into PDMS microdevices by combining proton beam lithography and conventional UV lithography fabrication techniques. This way, the microstructures and the microdevices can be made from the same material, which is not only useful, but in case of certain applications, it is essential. This work deals with the design of various microfluidic devices with and without integrated microstructures, for passive mixing purposes. The investigation involves the computer simulation and optimization, and then the fabrication of the chips with the above mentioned methods. Finally, the analysis of the mixing efficiency of the micromixer devices was realized with UV/vis spectroscopy at different fluid flow rates. Compared to the small size of the whole mixing chip, high mixing efficiency could be achieved.

1. Introduction

Microfluidic technology, which has been progressing steadily since 1979 when the first micro gas chromatograph was created [1], allows to perform many functions in one small chip, including mixing, reaction, separation, and analysis. Thanks to their small dimensions, their surface to volume ratio is extremely high. Because of this, they offer unique physical characteristics, very different ones from the macroscopic world. Important features of microfluidic devices are that they require small amount of reagent, increase reaction rates, and minimize sample handling. Generally, microfluidic devices are used in drug synthesis, gene analysis, and cell separation and sorting [2–4], among others.

At the same time, the Reynolds number of the fluid flow in them are typically below 1, so laminar flow dominates. This makes the mixing of two different solutions particularly difficult, and occurs only by diffusion. Therefore, the mixing is still a great challenge for researchers working with microfluidic devices. One type of microfluidic devices are, because of this, the micromixers, which are used to mix two or more solutions in a micro scale channel to handle micro and nanoliter volume of fluids. In general, micromixers can be classified into two types: active and passive [5–10]. In the mixing process, active micromixers need external force to create turbulence effects such as electrokinetics, dielectrophoretics, electrohydrodynamics, temperature, pressure, etc. [11–15]. Hence, the structures of active micromixers are often complicated. On the other hand the passive-type mixers can be easily fabricated, do not contain moving components, therefore they might be more interesting than active mixers, as reported in articles [16–19]. The flow in the micromixer is laminar, thanks to the micrometer-size channels, so the mixing occurs by molecular diffusion only. This process is generally slow, especially for macromolecules. Therefore, to achieve efficient mixing in micromixers based purely on diffusion, the molecular diffusion distance (channel cross dimensions) has to be reduced significantly [17].

Passive mixing devices rely entirely on fluid pumping energy and use special channel designs to restructure the flow in a way that reduces the diffusion length and maximizes the contact surface area [20–25]. Passive mixers were the first microfluidic devices reported, often entail less expense and more convenient fabrication than active micromixers, and can be easily integrated into more complex devices. The increase in the mixing efficiency is generally achieved by splitting the fluid stream using serial or parallel lamination [26,27], hydrodynamically focusing mixing streams[28], introducing bubbles of gas (slug) or liquid (droplet)

* Corresponding author. Institute for Nuclear Research (Atomki), H-4026, Debrecen, Bem tér 18/c., Hungary.
E-mail address: huszank@atomki.hu (R. Huszánk).

https://doi.org/10.1016/j.vacuum.2021.110295
Received 22 December 2020; Received in revised form 15 March 2021; Accepted 3 May 2021
Available online 9 May 2021

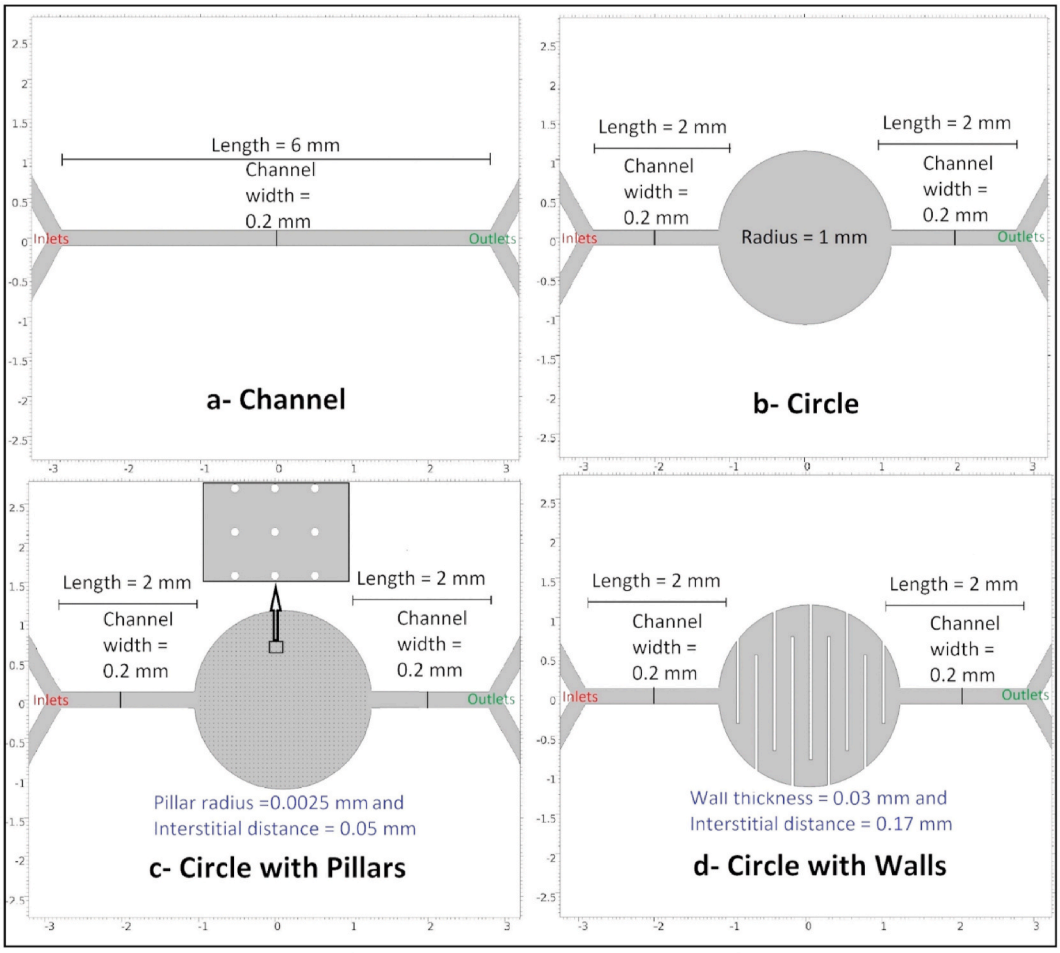

Fig. 1. Geometrical structure of different mixing unit area a) straight channel, b) circle, c) circle-with-pillars and d) circle-with-walls.

into the flow [29,30], or enhancing chaotic advection using ribs and grooves designed on the channel walls [31,32]. There are many studies for mixing-efficiency using passive micromixers with simple planar structures such as obstacles, unbalanced collisions, convergence–divergence channels and spiral channels etc. and their results shows acceptable range for efficiency 79–95% as mentioned in review article [33]. One of the most efficient passive micromixer, the so called staggered herringbone chaotic mixer, was fabricated using *PDMS* by a lithography process, in which a mixing efficiency of *99.7*% and *99.2%* was achieved at 20 μl/min and *at* 100 μl/min [34], respectively.

In this article, the performance characteristics of four different passive microfluidic mixer were studied, such as straight channel, empty circle, circle with pillars and circle with walls. The mixing efficiencies were simulated and the geometries of the microstructures were optimized using the COMSOL Multiphysics® software. The simple devices (straight channel, empty circle) were fabricated by UV lithography. In addition, the functionalization of these devices with 3D microstructures was obtained by the combination of the UV lithography and Proton Beam Writing techniques. The mixing efficiency of the fabricated micromixers were calculated from the concentrations of methylene blue test solutions measured using UV/vis spectrophotometry, at a range of flow rates.

2. Experimental

The Reynolds number,

$$Re = \frac{\rho u D_h}{\mu} = \frac{u D_h}{\nu} \quad (1)$$

Where ρ and μ are the fluid density and dynamic viscosity, respectively, ν is the kinematic viscosity, u is the velocity of fluid and D_h is the hydraulic diameter of the channel, distinguishes if the flow type is laminar or turbulent. The transition Re is generally expected to be in the range of 1500 and 2500 for most situations [35].

In our system, the calculated Re number, using Eq. (1), is from 0.21 to 3.06, depending on the actual design of the microstructures and the chip. Therefore the flow type is laminar in all cases.

2.1. Computational fluid dynamics (CFD) simulations

The CFD calculations were achieved with the microfluidics module of COMSOL Multiphysics (software version 5.3a). The geometries of the proposed two-dimensional designs are shown in Fig. 1. The main parts of micromixers are *2* inlet channels, *2* outlet channels and the mixing unit area. As shown in Fig. 1, all structures have the same geometry and number for inlets and outlets but have different mixing unit area like:

a straight channel, with length = 6 mm and width = 0.2 mm
b circle, with diameter = 2 mm
c circle-with-pillars, pillar diameter = 0.005 mm and spacing = 0.05 mm
d circle-with-walls, wall thickness = 0.03 mm and distance = 0.17 mm.

In this study, for evaluation of mixing performance, all proposed designs were simulated in COMSOL. The "creeping flow" and "transport of diluted species" modules were applied to perform the mixing simulations for two-dimensional designs. In cases of circle mixing area chips,

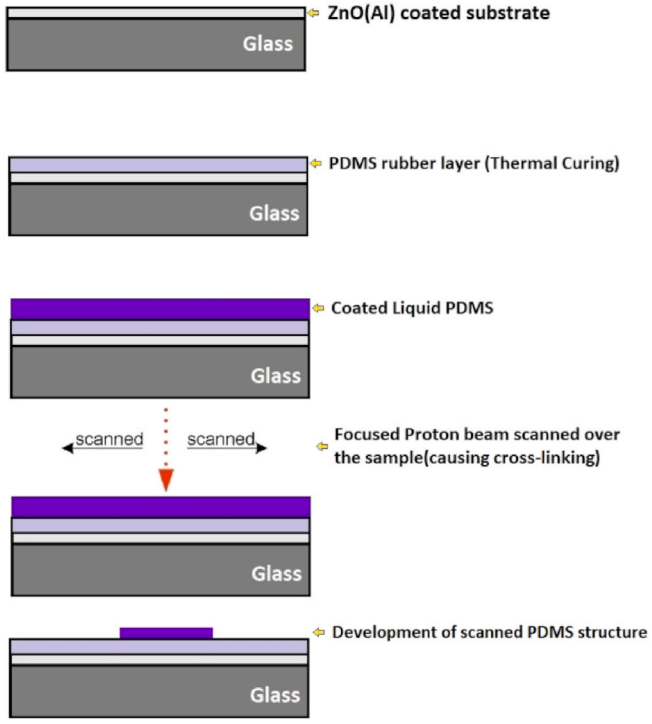

Fig. 2. Schematic illustration of the PBW process (side view). The proton beam was magnetically scanned over the resist at an area of 2 mm × 2 mm.

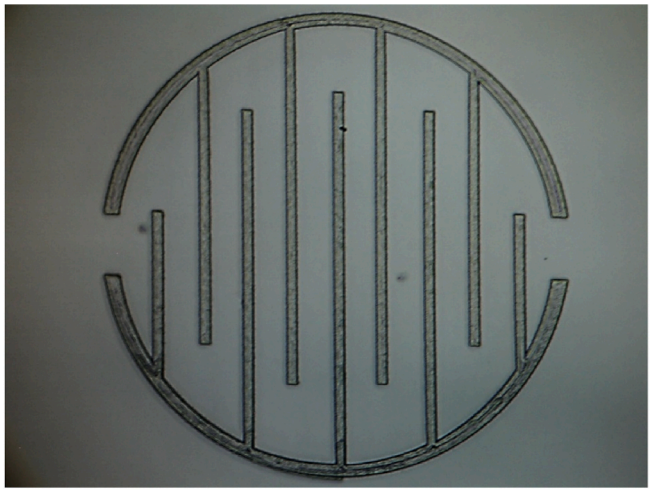

Fig. 3. Optical microscopic image of micromixer type circle with walls. Parameters: circle diameter: 2 mm; microwall thickness 0.03 mm, height 0.025 mm, distance 0.17 mm.

a short straight channel is also present, from the inlets to the mixing area, and from the mixing area towards the outlets, to make the chip fabrication feasible.

The governing equations in case of the flow of an incompressible Newtonian liquid in a micromixer are the Navier-Stokes and the continuity equation, presented in Eq. (2) and Eq. (3), respectively.

$$\nabla\left[-pI+\mu\left(\nabla u+(\nabla u)^{T}\right)\right]+F=0 \tag{2}$$

$$\rho\,\nabla(u)=0 \tag{3}$$

Where ρ is the fluid density, u is the flow velocity, μ is the dynamic viscosity of the fluid, p is the fluid pressure, I is the identity matrix, T is viscous stress tensor and F is the body force.

The species transport in the systems can be described by the convection – diffusion equation as shown in Eq. (4),

$$\nabla(-D\nabla c)+u\nabla c=R \tag{4}$$

Where c and D are concentration and diffusion constant of the species respectively and R is the source term.

2.2. Mixing efficiency

The Mixing Efficiency (M) of the micromixer applied in this study is defined using Eq. (5) 33,

$$M=1-\sqrt{\left(\frac{c_{out}-\overline{c}_{out}}{\overline{c}_{out}}\right)^{2}}\times 100\ \% \tag{5}$$

Where c_{out} is one of the outlet concentrations and $\overline{c}_{\mathrm{out}}$ is the average concentration of the two outlet concentrations. In accordance with Eq. (5), the mixing efficiency $M = 0\%$ indicates completely unmixed state of the species, while $M = 100\%$ indicates the completely mixed state. For practical applications, the acceptable range for efficiency of mixing is between *80 –100%*33.

2.3. Microfluidic chip fabrication

The chip fabrication includes the following steps:

1. Creation of PDMS base polymer rubber layer
2. Proton beam writing (PBW) of PDMS microstructures.
3. SU-8 photolithography of PDMS cap.
4. Bonding the PDMS cap onto the PDMS microstructures by plasma treatment.

2.3.1. Creation of PDMS base polymer rubber layer

As shown in Fig. 2, liquid PDMS mixture (Sylgard 184 kit, Dow-Corning, base polymer: curing agent volume ratio 10:1) is coated on a conductive glass substrate by a spin coater. It cross-linked on hotplate at temperature 85 °C for 30 min, forming about a 30 μm rubber layer.

2.3.2. Proton beam writing (PBW) of PDMS microstructures

In case of the micromixers, which use microstructures for mixing (i.e. micro pillars or walls), a new layer of about a 30 μm base polymer was spin-coated on the cross-linked rubber layer. This topmost liquid PDMS layer was applied as negative resist[36] for proton beam irradiation. The penetration depth of 2 MeV protons in PDMS is about 80 μm. This means that they transmit both the liquid and the rubber PDMS layer and stop in the glass substrate.

For the fabrication of the microstructures, proton beam writing method was applied, with a proton microprobe setup. The irradiations were carried out by 2.0 MeV protons with typically 500 pA beam current, focused down to 3 μm × 3 μm. The proton beam was magnetically scanned over the resist material according to the given scan pattern. These patterns include: micropillar array and circle with structured walls. The delivered fluence was between 3000 and 10000 nC/mm^2. The structures were developed directly after the irradiations with *tert*-butyl alcohol at 55 °C [36], then the samples were rinsed with ethanol to clean them. Fig. 3 shows the PDMS micro-walls created by PBW technique.

The PDMS changes chemically due to the proton irradiation because the methyl groups leave and cross-links form. Because of this, significant physical changes occur as well. Some of these changes were investigated earlier in detail [37,38]. In present work, only the structure geometries were considered.

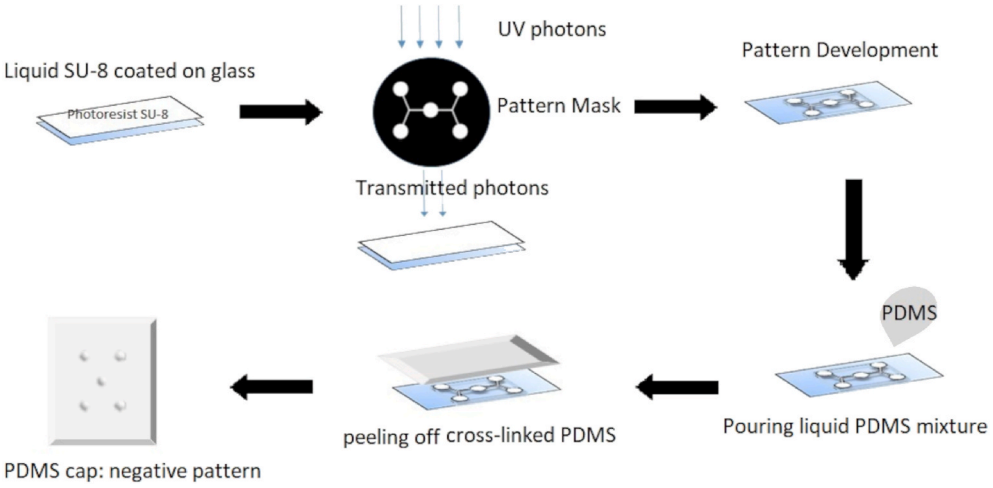

Fig. 4. Schematic description of PDMS cap formation using SU-8 master and UV lithography.

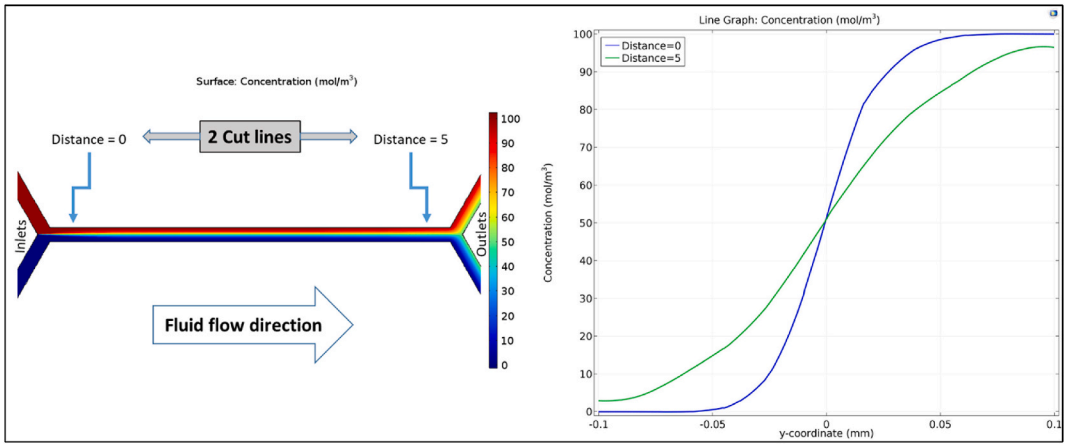

Fig. 5. Left: COMSOL simulation of mixing in channel structure. 2 cut lines at distance = 0 (near inlets) and distance = 5 (near outlets) are indicated. Right: Concentration profiles at the two cut lines.

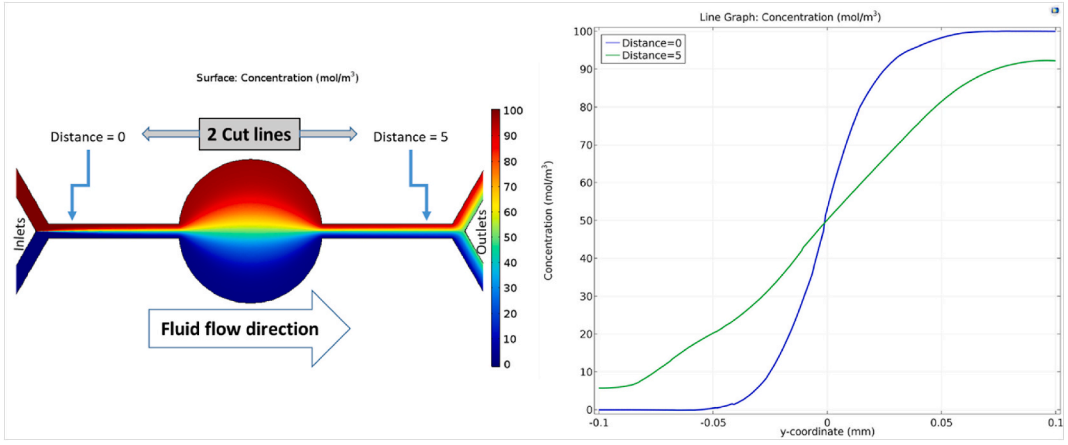

Fig. 6. Left: COMSOL simulation of mixing in circle structure. 2 cut lines at distance = 0 (near inlets) and distance = 5 (near outlets) are indicated. Right: Concentration profiles at the two cut lines.

2.3.3. SU-8 photolithography of PDMS cap

The cap of the chip was fabricated by photolithography, detailed in Fig. 4. A cleaned glass substrate is coated by SU-8 photoresist using spin coater. This was then irradiated by UV lamp through the cap mask. The UV photons induce cross-link formation and the UV irradiated areas solidify. Thereafter the SU-8 structure was developed. The PDMS mixture was poured on the SU-8 structure and let to crosslink. Finally, the formed PDMS cap was peeled off.

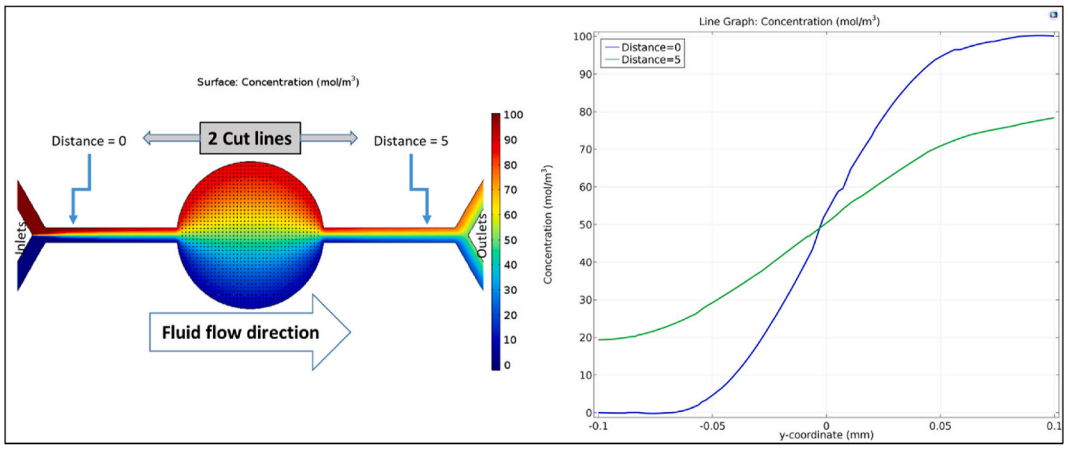

Fig. 7. Left: COMSOL simulation of mixing in circle-with-pillars structure. 2 cut lines at distance = 0 (near inlets) and distance = 5 (near outlets) are indicated. Right: Concentration profiles at the two cut lines.

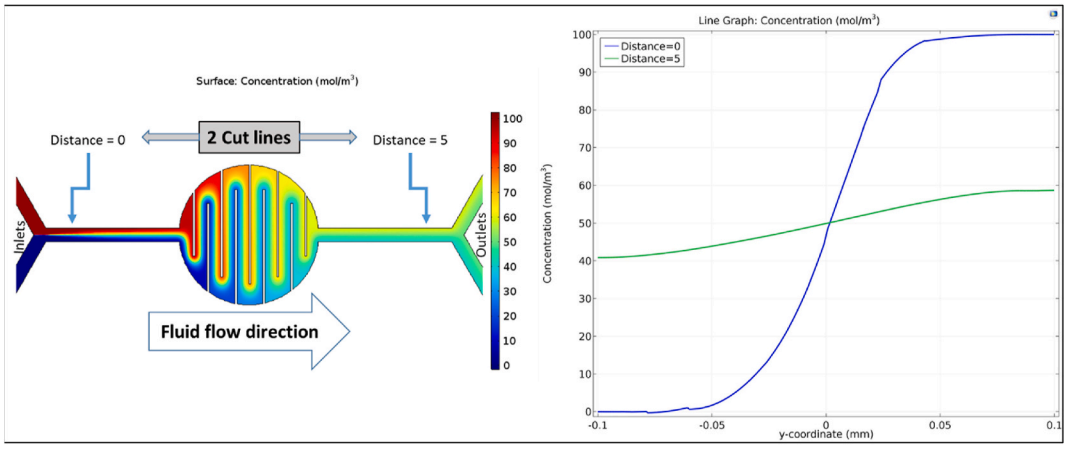

Fig. 8. Left: COMSOL simulation of mixing in circle-with-walls structure. 2 cut lines at distance = 0 (near inlets) and distance = 5 (near outlets) are indicated. Right: Concentration profiles at the two cut lines.

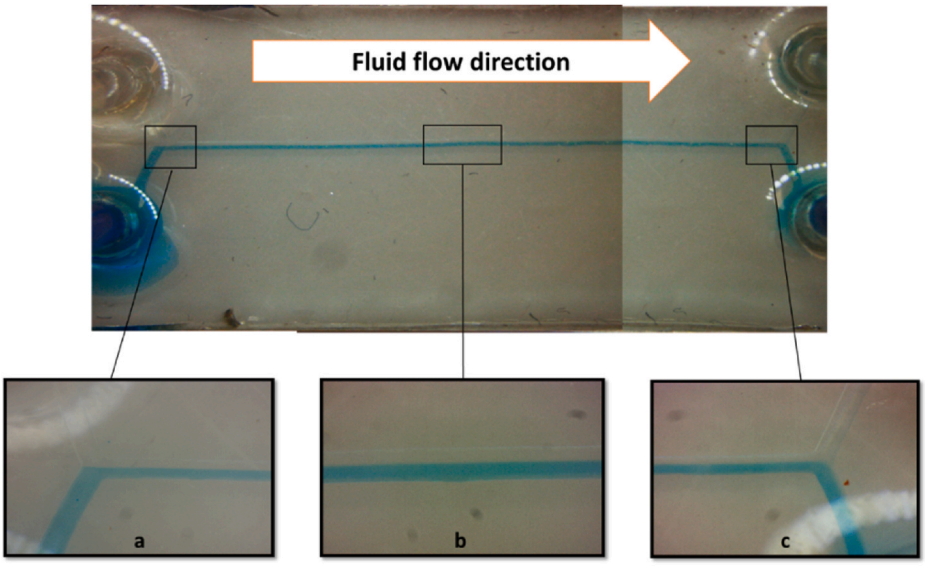

Fig. 9. Mixing level test of channel micromixer a) inlets portion, b) mixing channel portion and c) outlets portion.

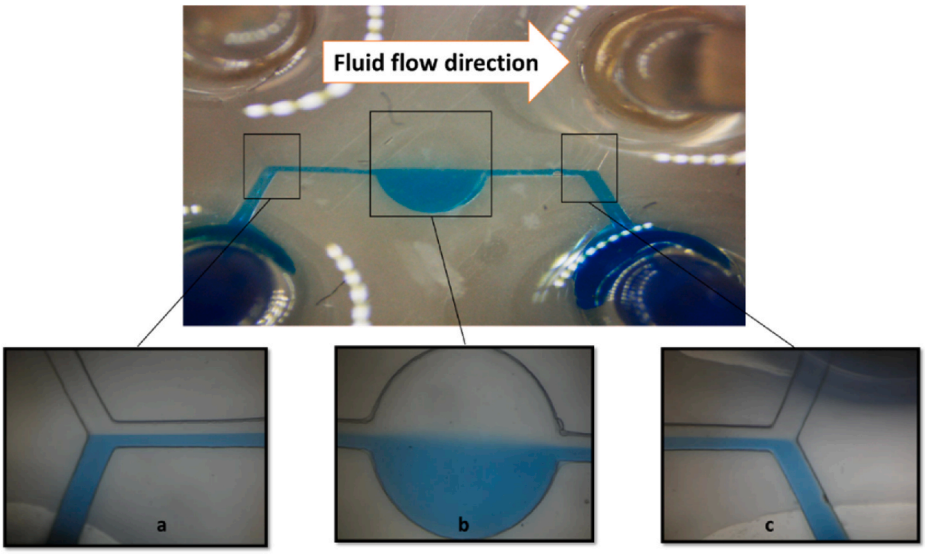

Fig. 10. Mixing level test of circle micromixer a) inlets portion, b) mixing circle portion and c) outlets portion.

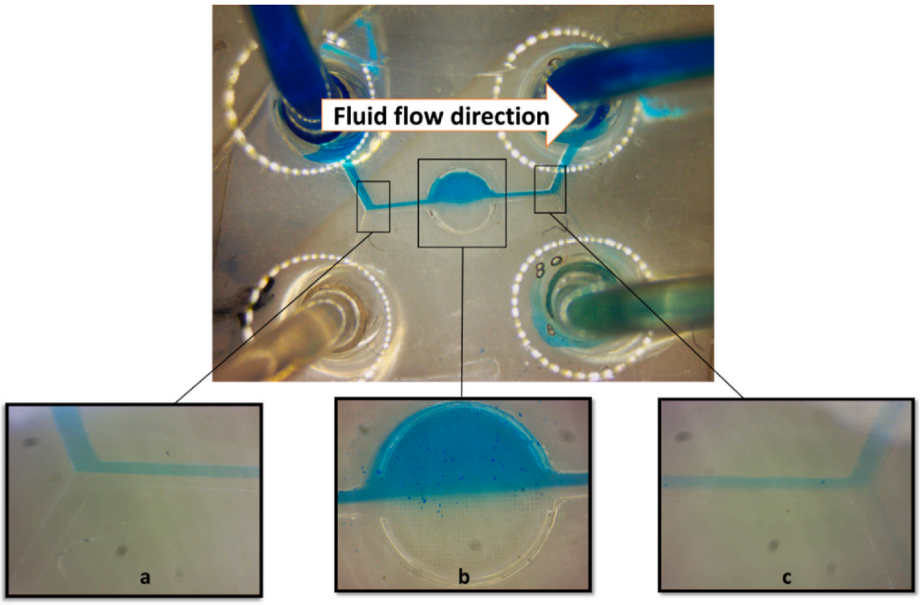

Fig. 11. Mixing level test of circle with pillars micromixer a) inlets portion, b) mixing circle with pillars portion and c) outlets portion.

2.3.4. Bonding the PDMS cap onto the PDMS microstructures by plasma treatment

The final form of microfluidic chip can be created by bonding the PDMS cap onto the PDMS microstructure pattern by plasma treatment. First the PDMS surfaces are chemically activated by air plasma, and then the two surfaces were aligned accordingly and squeezed. Afterwards, two inlet and two outlet holes were created into the cap. Finally, flexible tubes were connected to the inlets and the outlets.

3. Results and discussion

3.1. COMSOL simulation and mixing efficiency

In this paper, the mixing efficiencies of four different designs, illustrated in Fig. 1, were simulated using methods presented in Experimental. The value of molecular diffusion coefficient used in this model was fixed at 10^{-11} m^2/s. The concentration of the fluids entering the two inlets was set to *0* and 100 mol/m^3, indicated by blue and red colors respectively in Figs. 5–8. The model boundary conditions have a constant velocity of *0*.01 m/s at the two inlets. To find absolute concentrations before and after the mixing unit area, two cut lines were defined arbitrarily, close to the inlets and outlets, as they are indicated in Figs. 5–8.

The simulation results show that the mixing efficiency of the channel and the circle micromixers was low, as the edges of the green lines in Figs. 5–8 should tend toward 50 mol m^{-3} in case of perfect mixing. However, Fig. 7 shows that the mixing efficiency of circle with pillars was improved for the same conditions used for channel and circle micromixers, and the best mixing result was obtained using circle-with-walls structure as shown in Fig. 8.

From the concentration profiles one can see that the mixing efficiency can be significantly improved by using microstructures in microfluidic chips, especially in case of the micro walls structures.

The real chips were designed and fabricated based on these simulated designs. The less efficient chips were created as references.

The pressure drop for the simulated structures was calculated

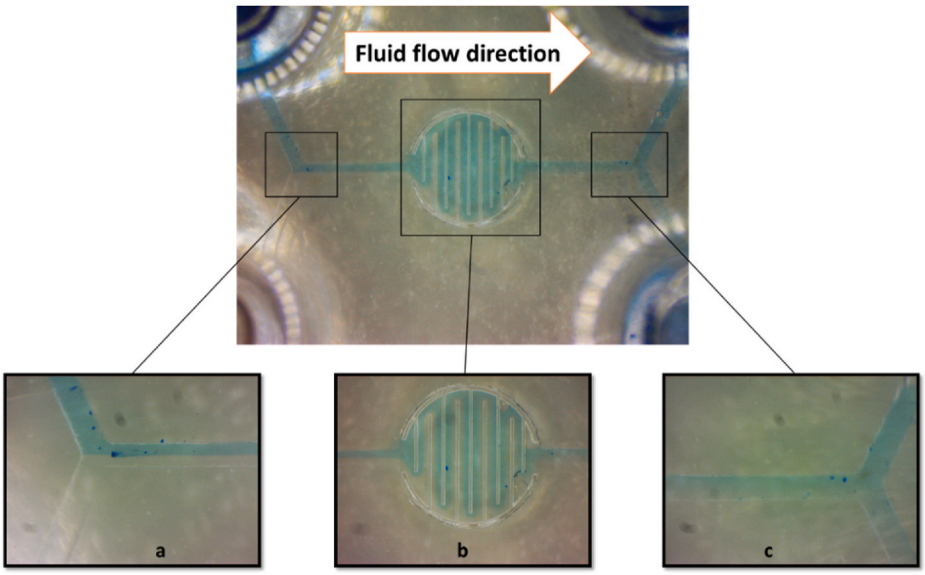

Fig. 12. Mixing level test of circle with walls micromixer a) inlets portion, b) mixing circle with walls portion and c) outlets portion.

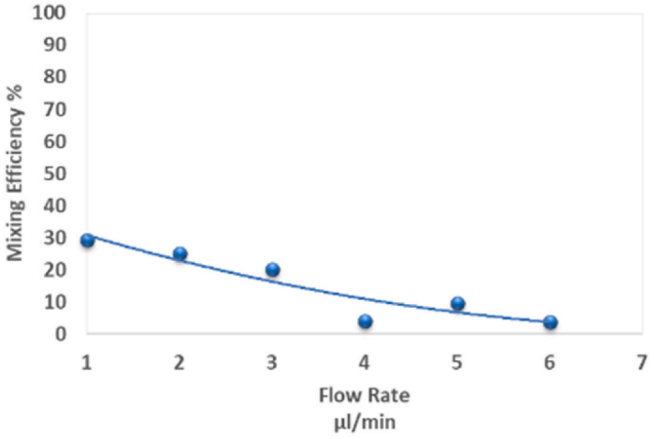

Fig. 13. Mixing efficiency vs. flow rate of channel micromixer.

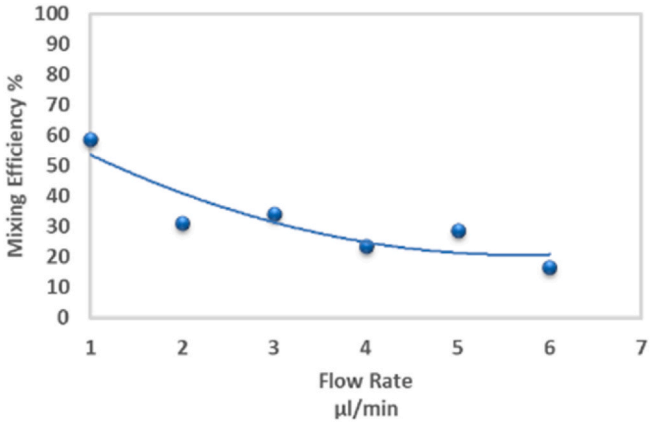

Fig. 14. Mixing efficiency vs. flow rate of circle micromixer.

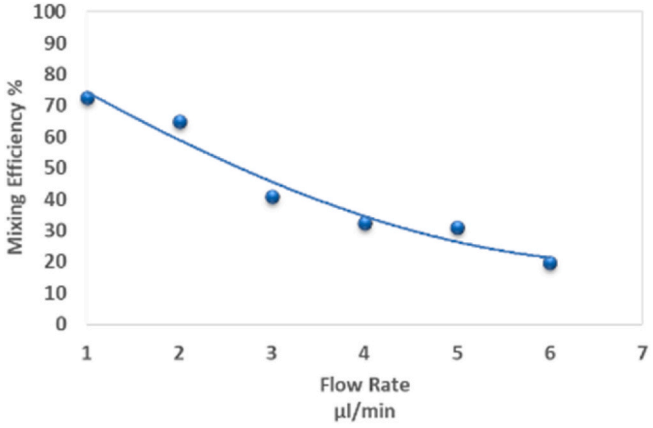

Fig. 15. Mixing efficiency vs. flow rate of circle with pillars micromixer.

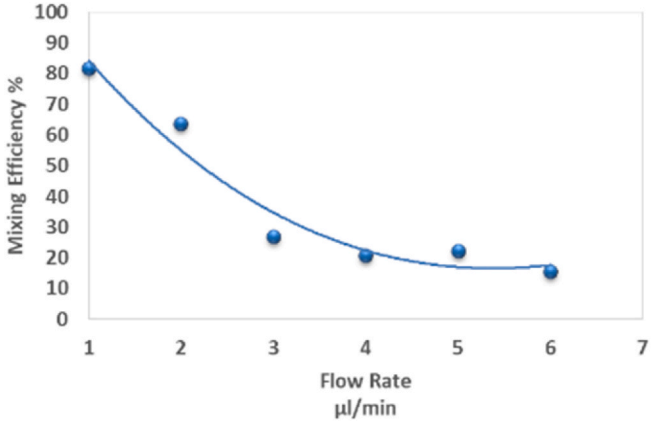

Fig. 16. Mixing efficiency vs. flow rate of circle with walls micromixer.

through the inlets and outlets for all the mentioned structures and its range was 0.139–1.74 kPa. For the real fabricated structures, the pressure drop was neglected due to the used low flow rates [39]. Low pressure drop is very important for industrial production because it decreases energy requirements.

3.2. Mixing test of the fabricated chips

To pump the two fluids at the inlets, a syringe pump was used with flow rates from *1* to 6 μl/min. Here we note, that the wetting ability of PDMS polymer changes dramatically due to ion irradiation depending on the ion dose, as can be seen in our earlier work for helium ions Huszánk et al. [37]. We suppose similar effect due to proton irradiation, because the chemical changes are similar but it cannot be estimated quantitatively, as the penetration depth of He ions are much smaller than that of protons, so energy deposition is much larger.

Since in these chips the liquids are pump driven, the surface forces can be neglected comparing the pumps.

All of the fabricated microfluidic chips of channel, circle, circle-with-pillars and circle-with-walls shown in Figs. 9–12 were tested to investigate the mixing efficiency. For the mixing test, two fluids, i) water and ii) very diluted aqueous solution of methylene blue, was used in the two inlets. In case of 100% mixing efficiency, exactly the half of the methylene blue concentration of the initial one is expected at both outlets. The concentrations of the methylene blue solutions were followed by spectrophotometry, in which the intensity change of an absorption peak (664 nm) was measured.

Figs. 9 and 10 shows that, mixing of the two fluids in the channel and in the circle micromixers were poor, as indicated all over the micromixer portion inlets, mixing unit area, and outlets. However, the mixing was seemingly improved by adding pillars inside the mixing unit area, as shown in Fig. 11. Finally, using walls inside the mixing unit area indicates mixing, as shown in Fig. 12.

3.3. Mixing efficiency calculations

First, the methylene blue concentrations at the two outlets of the chips were measured by UV/vis spectrophotometry. The mixing efficiencies were then calculated with Eq. (5), based on the differences in the concentrations at the two outlets.

For the calculations the density (ρ) and dynamic viscosity (μ) of water and methylene blue solution were considered equal because of the very low concentration of the latter (2×10^{-5} mol/dm [3]).

The mixing efficiencies were determined for flow rates from 1 to 6 μl/min using the four micromixer structures.

As illustrated in Figs. 13–16, the data show that the mixing efficiency decreases when the flow rate increases in case of all micromixers. At flow rate 1 μl/min, the mixing efficiency values were *29%*, *58%*, *72%* and *82%* for the micromixers channel, circle, circle-with-pillars and circle-with-walls, respectively. The highest mixing efficiency can be achieved using circle-with-walls micromixer structure, because its geometry increases the surface area between the different fluids and decreases the diffusion length. The experimental results follow the trend of the simulated results.

4. Conclusion

In this work, various microfluidic devices with and without integrated microstructures were designed, optimized and created for micromixing purposes (channel, circle, circle-with-pillars and circle-with-walls micromixers). As a new fabrication approach, poly(dimethylsiloxane) (PDMS) microstructures were integrated into PDMS microdevices by the combination of conventional UV lithography and proton beam lithography fabrication method. This way, the microstructures and the micro-devices can be made from the same material, which is important in case of certain applications. To compare the mixing capabilities of the proposed microstructure designs, real mixing tests were carried out. From the results of these tests, the mixing efficiencies were calculated and found to be 29%, 58%, 72% and 82% at flow rate 1 μl/min.

As a conclusion, we successfully integrated PDMS microstructures into PDMS microfluidic devices. With a proper design of the microstructures, the mixing efficiencies could be significantly improved, and reached as high as 82%, keeping the size of the chip in the order of a few millimetres. The presented method opens the opportunity to further improve mixing efficiencies and to further decrease chip dimensions, by the development of new designs and by fabricating smaller and finer structures by nano-lithography (nano sized proton beam lithography).

Declaration of competing interest

The authors declare that they have no known competing financial interests or personal relationships that could have appeared to influence the work reported in this paper.

Acknowledgement

This work was supported by the János Bolyai Research Scholarship of the Hungarian Academy of Sciences, the ÚNKP-19-4 New National Excellence Program of the Ministry for Innovation and Technology, and the European Regional Development Fund and Hungary in the frame of the project GINOP-2.2.1-15-2016-00012.

References

[1] S.C. Terry, J.H. Jerman, J.B. Angell, A gas chromatographic air analyzer fabricated on a silicon wafer, IEEE Trans. Electron. Dev. 26 (1979) 1880–1886.
[2] P. Yager, T. Edwards, E. Fu, K. Helton, K. Nelson, M.R. Tam, B.H. Weigl, Microfluidic diagnostic technologies for global public health, Nature 442 (7101) (2006) 412–418.
[3] G.M. Whitesides, The origins and the future of microfluidics, Nature 442 (7101) (2006) 368–373.
[4] B.H. Robertson, J.K. Nicholson, New microbiology tools for public health and their implications 1, Annu. Rev. Publ. Health 26 (2005) 281–302.
[5] A.D. Stroock, S.K.W. Dertinger, A. Ajdari, I. Mezić, H.A. Stone, G.M. Whitesides, Chaotic mixer for microchannels, Science 295 (2002) 647–651.
[6] L. Wang, J. Yang, P. Lyu, An overlapping crisscross micromixer, Chem. Eng. Sci. 62 (2007) 711–720.
[7] D.G. Hassell, W.B. Zimmerman, Investigation of the convective motion through a staggered herringbone micromixer at low Reynolds number flow, Chem. Eng. Sci. 61 (2006) 2977–2985.
[8] X. Fu, S. Liu, X. Ruan, H. Yang, Research on staggered oriented ridges static micromixers, Sens. Actuators, B 114 (2006) 618–624.
[9] H. Sato, S. Ito, K. Tajima, N. Orimoto, S. Shoji, PDMS microchannels with slanted grooves embedded in three walls to realize efficient spiral flow, Sens. Actuators, A 119 (2005) 365–371.
[10] C. Hong, J. Choi, C.H. Ahn, A novel in-plane passive microfluidic mixer with modified Tesla structures, Lab-on-a-Chip 4 (2004) 109–113.
[11] Z. Yang, S. Matsumoto, H. Goto, M. Matsumoto, R. Maeda, Ultrasonic micromixer for microfluidic systems, Sens. Actuators, A 93 (2001) 266–272.
[12] H.H. Bau, J. Zhong, M. Yi, A minute magneto hydro dynamic (MHD) mixer, Sens. Actuators, B 79 (2001) 207–215.
[13] J. Lin, K. Lee, G. Lee, Active mixing inside microchannels utilizing dynamic variation of gradient zeta potentials, Electrophoresis 26 (2005) 4605–4615.
[14] C. Tsouris, C.T. Culbertson, D.W. DePaoli, S.C. Jacobson, V.F. de Almeida, J. M. Ramsey, Electrohydrodynamic mixing in microchannels, AIChE J. 49 (2003) 2181–2186.
[15] L. Fu, R. Yang, C. Lin, Y. Chien, A novel microfluidic mixer utilizing electrokinetic driving forces under low switching frequency, Electrophoresis 5 (2005) 1814–1824.
[16] V. Hessel, S. Hardt, H. Löwe, F. Schönfeld, Laminar mixing in different interdigital micromixers: I. Experimental characterization, AIChE J. 49 (2003) 566–677.
[17] S.P. Sullivan, B.S. Akpa, S.M. Matthews, A.C. Fisher, L.F. Gladden, M.L. Johns, Simulation of miscible diffusive mixing in microchannels, Sens. Actuators, B 123 (2007) 1142–1152.
[18] J.B. Knight, A. Vishwanath, J.P. Brody, R.H. Austin, Hydrodynamic focusing on a silicon chip: mixing nanoliters in microseconds, Phys. Rev. Lett. 80 (1998) 3863–3866.
[19] F.G. Bessoth, A.J. deMello, A. Manz, Microstructure for efficient continuous flow mixing, Anal. Commun. 36 (1999) 213–215.
[20] Y. Liu, B.J. Kim, H.J. Sung, Two-fluid mixing in a microchannel, Int. J. Heat Fluid Flow 25 (2004) 986–995.
[21] A. Goullet, I. Glasgow, N. Aubry, Effects of microchannel geometry on pulsed flow mixing, Mech. Res. Commun. 33 (2006) 739–746.
[22] S. Park, J.K. Kim, J. Park, S. Chung, C. Chung, J.K. Chang, Rapid three-dimensional passive rotation micromixer using the breakup process, J. Micromech. Microeng. 14 (2004) 6–14.
[23] F. Jiang, K.S. Drese, S. Hardt, M. Küpper, F. Schönfeld, Helical flows and chaotic mixing in curved micro channels, AIChE J. 50 (2004) 2297–2305.
[24] S.H. Wong, M.C.L. Ward, C.W. Wharton, Micro T-mixer as a rapid mixing micromixer, Sens. Actuators, B 100 (2004) 359–379.

[25] H. Chen, J.-C. Meiners, Topologic mixing on a microfluidic chip, Appl. Phys. Lett. 84 (2004) 2193–2195.
[26] A. Kamholz, P. Yager, Molecular diffusive scaling laws in pressure-driven microfluidic channels: deviation from one dimensional Einstein approximations, Sensor. Actuator. B Chem. 82 (1) (2002) 117–121.
[27] N. Schwesinger, T. Frank, H. Wurmus, A modular microfluid system with an integrated micromixer, J. Micromech. Microeng. 6 (1996) 99.
[28] J. Knight, A. Vishwanath, J. Brody, R. Austin, Hydrodynamic focusing on a silicon chip: mixing nanoliters in microseconds, Phys. Rev. Lett. 80 (17) (1998) 3863–3866.
[29] A. Gunther, M. Jhunjhunwala, M. Thalmann, M. Schmidt, K. Jensen, Micromixing of miscible liquids in segmented gas- liquid flow, Langmuir 21 (4) (2005) 1547–1555.
[30] H. Song, J. Tice, R. Ismagilov, A microfluidic system for controlling reaction networks in time, Angew. Chem. 115 (7) (2003) 792–796.
[31] T. Johnson, D. Ross, L. Locascio, Rapid microfluidic mixing, Anal. Chem. 74 (1) (2002) 45–51.
[32] A. Stroock, S. Dertinger, A. Ajdari, I. Mezic, H. Stone, G. Whitesides, Chaotic mixer for microchannels, Science 295 (5555) (2002) 647.
[33] G. Cai, L. Xue, H. Zhang, J. Lin, A review on micromixers, Micromachines 8 (2017) 274.
[34] Xueye Chen, Wang Xiaolei, Optimized modular design and experiment for staggered herringbone chaotic micromixer, Int. J. Chem. React. Eng. 13 (3) (2015) 305–309.
[35] N. Nguyen, S. Wereley, Fundamentals and Applications of Microfluidics, Artech House, Norwood, 2002.
[36] R. Huszank, I. Rajta, Cs Cserháti, Direct formation of high aspect ratio multiple tilted micropillar array in liquid phase PDMS by proton beam writing, Eur. Polym. J. 69 (2015) 396–402.
[37] R. Huszank, D. Szikra, A. Simon, S.Z. Szilasi, I.P. Nagy, $^{4}He^{+}$ ion beam irradiation induced modification of poly(dimethylsiloxane). Characterization by infrared spectroscopy and ion beam analytical techniques, Langmuir: ACS J. Surf. Colloids 27 (7) (2011) 3842–3848. Apr.
[38] R. Huszank, A. Bonyár, J. Kámán, E. Furu, Wide range control in the elastic properties of PDMS polymer by ion beam (H^{+}) irradiation, Polym. Degrad. Stabil. 152 (2018) 253–258.
[39] V. Viktorov, M.R. Mahmud, C. Visconte, Comparative analysis of passive micromixers at a wide range of Reynolds numbers, Micromachines 6 (8) (2015) 1166–1179.